ACS OMEGA

Article

Cite This: ACS Omega 2019, 4, 3812−3819

http://pubs.acs.org/journal/acsodf

Enhanced NO_2 Sensing at Room Temperature with Graphene via Monodisperse Polystyrene Bead Decoration

Haifeng Fei,[†] Gang Wu,[‡] Wei-Ying Cheng,[§] Wenjie Yan,[†] Hongjun Xu,[†] Duan Zhang,[∥] Yanfeng Zhao,[†] Yanhui Lv,[†] Yanhui Chen,[⊥] Lei Zhang,[#] Cormac Ó Coileáin,[†] Chenglin Heng,[†] Ching-Ray Chang,*[,¶] and Han-Chun Wu*[,†]

[†]School of Physics, Beijing Institute of Technology, Beijing 100081, P. R. China

[‡]School of Materials Science and Engineering, Tongji University, Shanghai 201804, P. R. China

[§]Graduate Institute of Applied Physics and [¶]Department of Physics, National Taiwan University, Taipei 106, Taiwan

[∥]Elementary Educational College, Beijing Key Laboratory for Nano-Photonics and Nano-Structure, Capital Normal University, Beijing 100048, P. R. China

[⊥]Institute of Microstructure and Property of Advanced Materials, Beijing University of Technology, Beijing 100124, China

[#]School of Chemical Engineering and Technology, Tianjin University, Tianjin 300072, P. R. China

Supporting Information

ABSTRACT: Graphene is a single layer of carbon atoms with a large surface-to-volume ratio, providing a large capacity gas molecule adsorption and a strong surface sensitivity. Chemical vapor deposition-grown graphene-based NO_2 gas sensors typically have detection limits from 100 parts per billion (ppb) to a few parts per million (ppm), with response times over 1000 s. Numerous methods have been proposed to enhance the NO_2 sensing ability of graphenes. Among them, surface decoration with metal particles and metal-oxide particles has demonstrated the potential to enhance the gas-sensing properties. Here, we show that the NO_2 sensing of graphene can be also enhanced via decoration with monodisperse polymer beads. In dark conditions, the detection limit is improved from 1000 to 45 ppb after the application of polystyrene (PS) beads. With laser illumination, a detection limit of 0.5 ppb is determined. The enhanced gas sensing is due to surface plasmon polaritons excited by interference and charge transfer between the PS beads. This method opens an interesting route for the application of graphene in gas sensing.

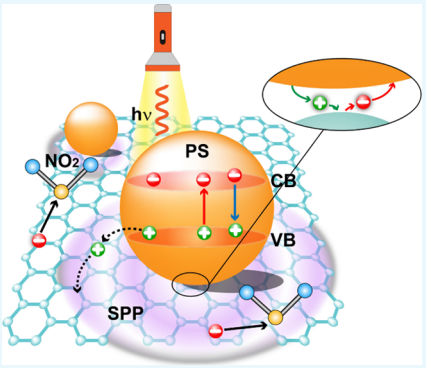

1. INTRODUCTION

Toxic gases such as NH_3, CO, NO_2, and SO_2, which are largely derived from factories and vehicles, can inflict great long-term harm on the environment and human health.[1] Among these gases, nitrogen dioxide (NO_2) is one of the most hazardous, which can cause damage to the lungs, cardiovascular system, and upper respiratory tract when as little 53 parts per billion (ppb) NO_2 is inhaled.[2,3] Therefore, it is essential to develop high-performance gas sensors with ultra-sensitive properties to monitor the concentration of NO_2 for both the environment and human health. There is a profusion of research on metal oxides,[4−9] conducting polymers,[10] and related heterojunctions, etc.[11] However, gas sensors based on metal oxides have several drawbacks, such as low sensitivity at room temperature (RT), poor selectivity, high power consumption, and complex synthesis techniques, which limit their application for NO_2 detection.[12,13] Furthermore, in spite of their RT operation and ease of processing, the effects of humidity and degradation limit the application of conducting polymers for gas sensing.[14]

Graphene is a honeycomb-like two-dimensional monoatomic layer with many excellent properties.[15,16] Over the past years, graphene has received ever more attention for applications in gas sensing[17] because of its large surface area (2630 m^2/g) and extraordinarily high charge carrier mobility (15 000 $cm^2\ V^{-1}\ s^{-1}$) at RT.[18] The superiority of graphene for gas sensing relies on two basic factors associated with its 2 dimensional nature, that is, the ultrahigh surface area per atom and high electron transport along the graphene base-plane.[19] A wide range of chemicals, biomolecules, and gas/vapors have been detected using graphene-based sensors.[20−22] It is reported that chemical vapor deposition (CVD)-grown graphene has a detection limit (DL) of 100 ppb with an absorption time of 1000 s.[20] A graphene-based field-effect transistor gas sensor has been reported to have a sensitivity of 2.5 ppm.[23] Multilayer graphene has been shown to have a DL

Received: December 17, 2018
Accepted: February 6, 2019
Published: February 21, 2019

DOI: 10.1021/acsomega.8b03540
ACS Omega 2019, 4, 3812−3819

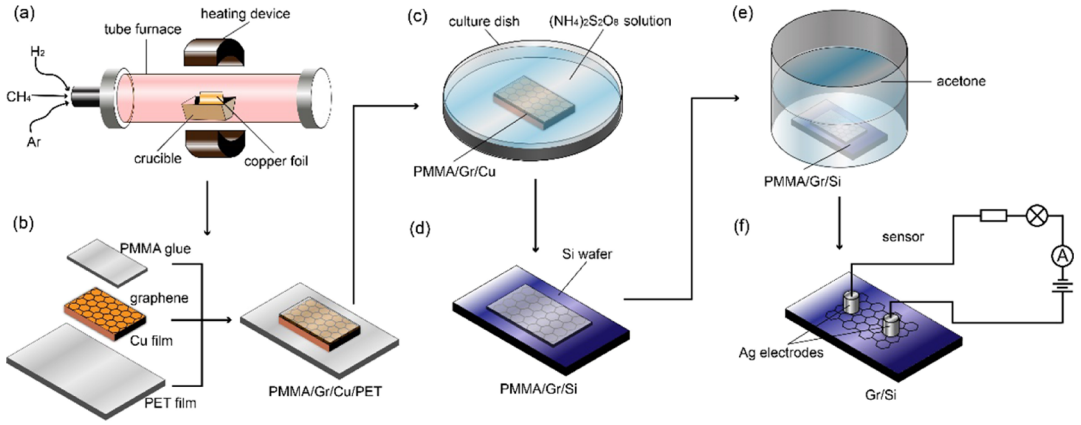

Figure 1. Graphene gas sensor fabrication. (a) Schematic drawing of graphene synthesized by CVD. (b) Graphene coated with PMMA for transfer. (c) Removal of graphene from Cu foil. (d) Transferred to the Si substrate with 300 nm SiO_2 with PMMA (e) PMMA removal with acetone. (f) Schematic drawing of graphene gas sensor.

of 1 ppm ppb with an absorption time of 1800 s.[24] Several methods have been proposed to enhance the NO_2 sensing capability of graphene by improving the interactions between graphene and the NO_2 molecules, such as ozone-treatment[25] and the introduction of defects and dopants.[26] Decorating graphene with metal,[27,28] metal oxide nano-particles,[29−31] and polymers[32−34] has proved to be a potential approach for enhancing its gas sensing properties. These graphene hybrids with modulated electronic properties enhance the selectivity and sensitivity. Polystyrene (PS) beads are micrometer-sized monodisperse polymer particles. It was reported recently that by introducing PS beads on graphene, surface plasmon polaritons (SPPs) waves are excited in the graphene through diffraction of the light, which significantly enhances the interaction between the graphene and molecules.[35]

In this work, PS beads were drop-coated onto the surface of graphene. We found that the charge transfer between PS beads and graphene and the excited SPP waves through diffraction of light by the PS beads significantly enhance the NO_2 sensing. A clear response is measured for 45 ppb NO_2 after PS bead decorating in dark conditions. With the illumination of a laser, an ultra-high DL of 0.5 ppb is achieved. Moreover, several localized domains are mapped under the microscope to investigate the impact the arrangement of the PS beads on the graphene. Our results indicate that when the graphene is decorated by submonolayer, PS bead enhancement increases with PS bead coverage density but the response decreases with increasing layer thickness. This research may open an interesting window for the study graphene-based gas sensors.

2. RESULTS AND DISCUSSION

Graphene was synthesized on Cu foil via CVD.[36] To synthesize the large-scale continuous monolayer graphene, Cu foil was folded into a pocket after Ar plasma treatment (Figure 1a). To further remove surface oxidization and contamination, the Cu pocket was annealed at 1035 °C for 40 min with a hydrogen flow rate of 10 sccm prior to growth. The graphene growth was carried out at 1035 °C for 40 min under a methane and a hydrogen flow. Details of the growth can be found elsewhere.[35] After synthesis, the external surface of the pocket was etched by oxygen plasma. As shown in Figure 1b, the inner surface of the pocket was coated with polymethylmethacrylate (PMMA) to form a stamp during transfer. The copper was etched away by soaking in ammonium persulfate solution for 6 h (Figure 1c). The floating PMMA/graphene stack was soaked in deionized water for 30 min, and then transferred onto a Si wafer with 300 nm SiO_2 (Figure 1d). The PMMA was then dissolved using acetone (Figure 1f). Silver wires were used as electrodes for gas sensing.

Figure S1a shows the optical image of the graphene after transfer. No clear residue is observed. The quality of the graphene after transfer was further characterized with Raman spectroscopy. Figure S1b shows the Raman spectra of the graphene on a SiO_2 substrate using an excitation wavelength of 532 nm. A strong G band located at 1591 cm^{-1} and a sharp and symmetric 2D band at 2684.5 cm^{-1} are present. The sharpness of the peaks and the intensity ratio (2:1) of 2D to G Raman bands indicate that the graphene is monolayer in nature and of high quality.[37] PS beads were deposited onto the graphene surface by a drop-coating method using a pipette, as shown in Figure 2a. Before drop-coating, PS beads were diluted with a mixture of alcohol and water. Figure 2b,c shows typical scanning electron microscopy (SEM) and transmission electron microscopy (TEM) images, respectively, for PS beads on a graphene surface. The PS beads have a uniform diameter of ∼1 μm and the coverage of PS beads can have various configurations, that is, areas without PS beads, with few PS beads, with a monolayer PS beads, and with multilayers PS beads. X-ray photoemission spectroscopy (XPS) was further used to investigate the decoration of PS beads on the graphene. Figure 2d shows XPS compositional analysis of the bare graphene and the graphene decorated with PS beads. For the graphene on a SiO_2 substrate, the binding energy for C 1s is 284.33 eV. However, for the graphene decorated with PS beads, because of a significant charge transfer between the graphene and PS beads, the C 1s peak moves to 284.82 eV. It also indicates that the graphene surface is truly decorated with PS beads.

The dynamic-sensing response of the graphene sensor was investigated by detecting NO_2 in dry air at RT. A constant source−drain bias of 1 V was applied to the sensor and the electrical resistance change of the device upon exposure to NO_2 was monitored and recorded as the sensing signal. Figure 3a shows the dynamic-sensing response of a graphene sensor before the drop-coating of the PS beads. The concentration of NO_2 varies from 45 to 100 000 ppb. There is a clear signal starting at 1 ppm with a sensitivity of 2%. The sensitivity (S) is

DOI: 10.1021/acsomega.8b03540
ACS Omega 2019, 4, 3812−3819

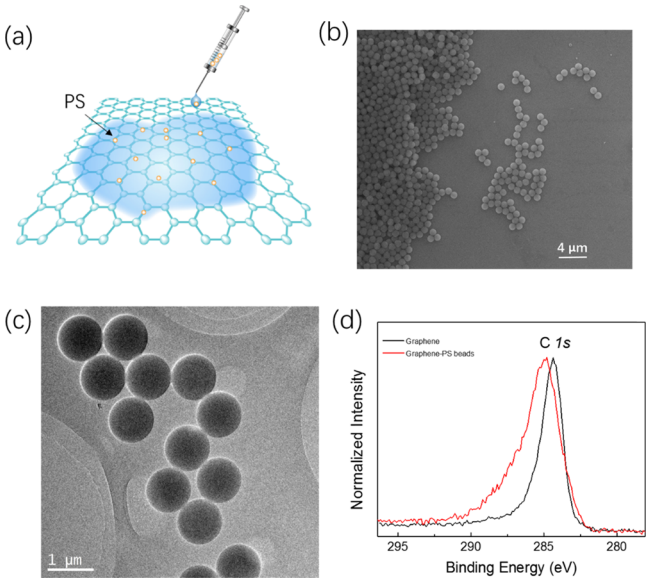

Figure 2. Characterization of graphene decorated with PS. (a) Schematic drawing of drop-coating a lower density of PS beads onto the graphene using an injector pipette. (b) SEM image of the graphene decorated with PS beads. (c) TEM image of the graphene decorated with PS beads. (d) XPS compositional analysis of bare graphene and the graphene decorated with PS beads.

defined as, $S = \Delta R/R_0 \times 100\%$, where $\Delta R = R - R_0$, R_0 and R are the electrical resistances of the sensor in air before a sensing cycle and the target gas, respectively. The resistance of the sensor decreases with increasing NO_2 concentration, indicating the p-type characteristics of the graphene and NO_2 working as an electron acceptor. When NO_2 is adsorbed onto the surface of graphene, electrons will be transferred from the graphene to the NO_2 molecules, which increases the hole concentration in the graphene and thus decreases the resistance. Figure 3b shows the dynamic-sensing response of the graphene sensor measured in dark conditions after PS bead drop-coating. Magnified gas sensing dynamics under each gas concentration is shown in Figure S2. Note, the sensor was pumped in vacuum for half an hour to aid the removal of molecules adsorbed on the surface. The resistance decreases by around 10% when the graphene is decorated with PS beads, indicating that a significant portion of electrons have been transferred from the graphene to the PS beads at the interface between the graphene and PS beads. This is consistent with the XPS characterization (Figure 2d). Remarkably, a signal from 45 ppb with a sensitivity of 0.8% is clearly observed. The NO_2-sensing performance of the graphene can be further enhanced by photo-illumination. The dynamic-sensing response of the PS bead-coated graphene sensor measured under 635 nm photo-illumination is plotted in Figure S3. A sensitivity of 2% was achieved when the device was exposed to 45 ppb NO_2 under 635 nm photo-illumination, which is around a 2.5 times performance enhancement compared to that without photo-illumination. Similar enhancement behavior was observed for other wavelengths. Figure 3c summarized the sensing responses of the graphene sensor to 45 ppb NO_2 under various conditions. One can see that no response is detected for sensors based on the pristine graphene in darkness. After decoration with PS beads, a sensitivity of 0.45% is achieved in the dark, and this can be further enhanced to 1% under 1064 nm photo-illumination. Thus, PS bead decoration significantly enhances the NO_2 sensing of graphene. A very low DL of 45 ppb is achieved with little noise, providing scope for further improvement. Extrapolating, the ideal DL is around 0.5 ppb, which is calculated by considering the noise and the slope of the sensitivity versus concentration.[38] The excellent sensing response is competitive when compared with most other high-performance NO_2 gas sensors. For example, the single-layered graphene has a DL of 2.5 ppm at RT.[23] Cu-modified carbon spheres/reduced graphene oxide has a DL of 10 ppm at RT.[39] The lower DL of voltage-activated reduced graphene oxide is around 50 ppb,[40] for further comparison, the DLs of more graphene-based NO_2 gas sensors are summarized in Table 1.

The long-term stability and repeatability of the sensor is very important for its application.[41] Figure 3d shows the dynamic-sensing responses of the same sensor under 1064 nm laser illumination measured as fabricated and after 4 month air exposure. The sensor still works properly after 4 month air exposure but with a sensitivity reduced by 25%. The reduced sensitivity is mainly due to the adsorption of other gas molecules when exposed to air. In addition, multicycle dynamic sensing responses were used to demonstrate the stability of the sensor (Figure S4). It can be seen that our sensor fully saturated in 8 h and the sensitivity of the sensor has a fluctuation of 0.12% for 8800 ppb NO_2. Figure 3e shows the effect of humidity on the sensing response of the gas sensor. The response increases with increasing humidity, suggesting that the presence of water does not degrade performance but that the humidity must be monitored concurrently for real applications. For the application of a sensor in a real environment, selectivity, the ability to discriminate the target gas of interest in the presence of other gases, is also very important. To investigate this, a graphene sensor decorated with PS beads was exposed to a variety of gases at a concentration of 1 ppm, including NO_2, H_2S, NH_3, and CO. Figure 3f summarizes the responses to these gases. The sensitivity is around 3% when exposed to 1 ppm NO_2. While when exposed to 1 ppm H_2S, the sensitivity is less than 0.2% and no response was detected for 1 ppm CO or NH_3. Thus, the sensors showed a lower response to these possibly interfering gases relative to the NO_2.

To further investigate the effect of PS beads on the NO_2-sensing capability of the graphene under photo-illumination, we fabricated a single sensor with four different PS distribution densities (Figure 4a). Figure 4b shows representative SEM images for four distinct areas, that is, an area without PS (area 1), with few PS beads (area 2), with monolayer PS beads (area 3), and with multilayers PS beads (area 4). A low-magnification SEM image of the areas in Figure 4b is shown in Figure S5, and the areas 1−4 with different PS bead distributions are clearly marked. Figure S6 is a typical photographic image of one of our devices. The dynamic-sensing response of the graphene sensor was investigated by locally illuminating each of the four areas with 1064 nm laser under a microscope. In other words, the resistance of the overall device was determined for local illumination in each of the four areas. For example, to investigate the effect of the PS beads in area 2 under photo illumination we focused the laser beam to the area 2. The diameter of the laser spot was around 10 μm. Figure 4c shows the dynamic-sensing response of the graphene sensor when locally illuminated in those four areas. For comparison, the dynamic-sensing response of the unilluminated sensor is plotted as well, and it is clear that photo-illumination can enhance gas-sensing response (Figure

DOI: 10.1021/acsomega.8b03540
ACS Omega 2019, 4, 3812−3819

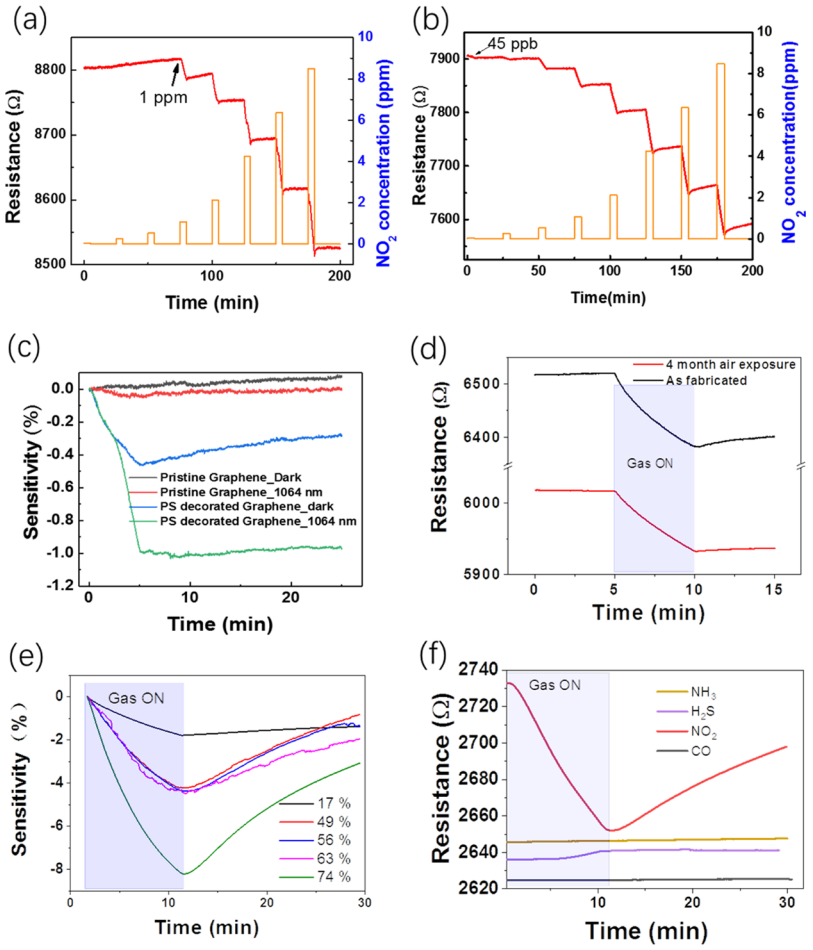

Figure 3. Graphene NO_2 sensing enhanced by PS decoration. (a) Gas-sensing dynamics of graphene-based gas sensor before and (b) after drop coating with PS beads. (c) Sensing responses of the graphene sensor for 45 ppb NO_2 for illumination and decoration conditions. (d) Dynamic-sensing responses of the same sensor measured as fabricated and measured after 4 month air exposure under 1064 nm laser illumination. (e) Dynamic-sensing responses of a sensor for 4400 ppb NO_2 at different humidities. (f) Dynamic-sensing responses of a PS/graphene sensor for a variety of gasses at 1 ppm.

Table 1. Summary of Recent Research studies about the Graphene-Based NO_2 Sensor at RT

sensing material	working temperature	LOD	sensitivity	reference
rGO/CuO	RT	1 ppm	14% $((I_g - I_a)/I_a)$	30
rGO	RT	50 ppb		40
rGO/Ag NWs	RT	50 ppm	15% <keep-together>$((R_g - R_{N_2})/R_{N_2})$</keep-together>	45
Cu@CS/rGO	RT	10 ppm	16% $(\|R_g - R_a\|/R_a)$	39
rGONMFs	RT	1 ppm	13.6% $(\|R_g - R_0\|/R_0)$	46
Gr	RT	100 ppb	4% $((R - R_0)/R_0)$	20
single-layered Gr	RT	2.5 ppm		23
ozone-treated Gr	RT	1.3 ppb		25
rGO/NiO	200 °C	1 ppm	200% $((R - R_0)/R_0)$	47
rGO + PVP	RT	20 ppm		48
printed rGO/S + Ag	RT	50 ppm	74.6% $((R - R_0)/R_0)$	49
rGO/hydrazine + ZnO	RT	5 ppm	25.6% $((R - R_0)/R_0)$	50
GO + Cs	RT	90 ppb		51
rGO/$NaBH_4$	RT	5 ppm	11.5% $((R - R_0)/R_0)$	52
Gr/PS	RT	45 ppb	2% $((R - R_0)/R_0)$	this work

4d). In addition, the enhancement increases with PS bead coverage density but decreases with increasing layer thickness. In area 4, the multilayer of PS beads is too thick for the laser to efficiently penetrate, resulting in a decrease in sensitivity. We also fitted the adsorption sections of the response curve with the expression $y = y_0 + A\, e^{x/\tau_A}$, where τ_A is the adsorption time (response time). Figure S7 shows the adsorption time changes with the concentration of PS beads. The adsorption time τ_A decreases with PS bead density but increases with increasing layer thickness. To further investigate the effect of PS bead

DOI: 10.1021/acsomega.8b03540
ACS Omega 2019, 4, 3812−3819

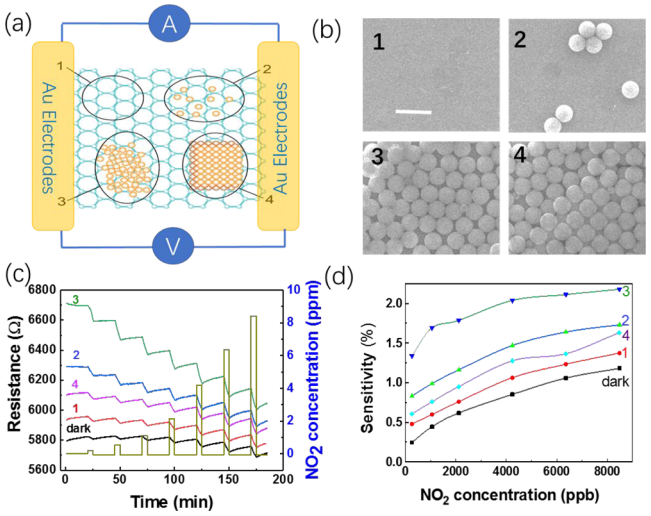

Figure 4. Sensing performance of the graphene gas sensor with localized illumination for four distinct PS bead coverage densities. (a,b) are schematic drawing and SEM images of the graphene with four PS beads distributions. The scale bar is 2 μm. (c) Dynamic-sensing response in dark and with four areas of localized 1064 nm light illumination (d) and corresponding sensitivity.

coverage density, we fabricated four sensors with four different densities. Figure S8 shows the dynamic-sensing response of four graphene sensors with different PS concentrations measured in dark against 250 ppb NO_2. Again, it is found that the enhancement also increases with PS bead coverage density but decreases with increasing layer thickness. For multilayers of PS beads, NO_2 molecules will prefer to adsorb on the top PS beads covering the graphene, which decreases the charge transfer between graphene and bottom PS beads. Thus, resulting in the decrease in sensitivity.

There are four main ways to enhance the gas sensitivity of the graphene and increase the interaction between the gas molecules and graphene: (1) changes in conductance of the graphene by redistribution of electrons; (2) providing electrons or holes to change the carrier concentration of the graphene; (3) covalent bond formation between the gas molecules and graphene;[42] and (4) extra surface area within concave regions between the graphene and PS beads. Figure 5 shows a schematic drawing of the charge transfer and electron distribution of graphene/PS bead hybrids under photo-illumination. It has been shown in finite difference time domain simulations that the maximum field enhancement factor (E^2/E_{inc}^2) is around 2.25 in the graphene/PS bead hybrid, where E_{inc} is the incident electric field of the incident light and E is the total local electric field in the presence of the PS particle.[35] The calculated maximum field enhancement factor is slight smaller than the measured gas-sensing enhancement factor of 2.5 under photo-illumination. The simulations also show that localized oscillations appear in the graphene emanating from the contact point. The SPP wave propagation along the graphene layer will also contribute the gas-sensing enhancement. To confirm the presence of the SPP wave in the graphene, the Raman spectra of the four positions marked in Figure 4b were investigated (Figure 5b). Several new peaks appear apart from the strong G band and the symmetric 2D band of graphene, which correspond to the Raman modes of isotactic and atactic PS beads.[43] Note, area 1 does not contain any PS beads and should not have PS-related peaks. However, areas 1−4 are all on the same sample as shown in Figure S5. Thus, when the Raman laser is focused on area 1, it is possible for light to scatter onto nearby PS beads producing a stray signal, thus the spectra of area 1 will include weak PS peaks. Interestingly, the intensity of the G band does not change significantly with the introduction of PS beads, indicating PS bead decoration will not change the quality of the graphene. In contrast, the 2D band is significantly enhanced with PS bead decoration. An enhancement factor of 2 is achieved at position 3. With increasing the layer thickness, the enhancement factor decreases which is consistent with the gas-sensing measurements. It is known that the 2D band in the graphene reflects the electron distribution and doping in the graphene.[44] The enhanced 2D band suggests that PS bead decoration excites SPP waves and

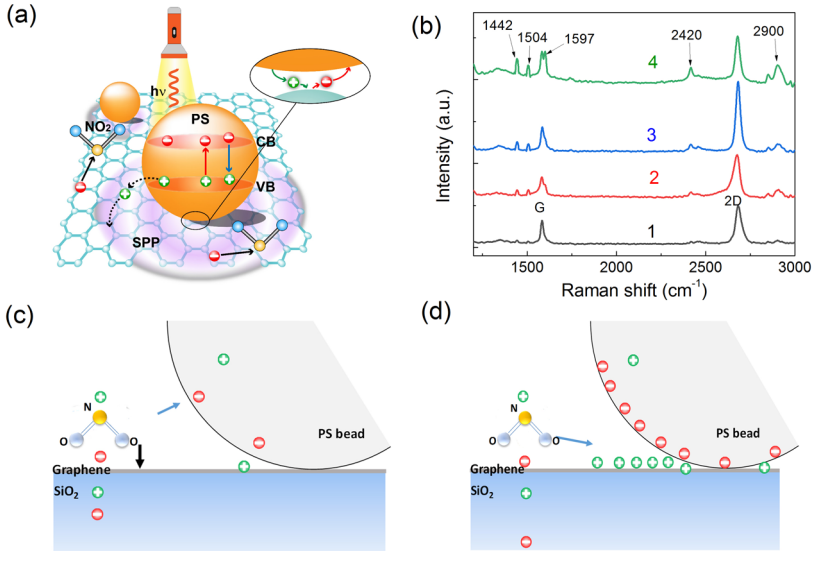

Figure 5. (a) Schematic drawing of charge transfer and electron distribution of graphene/PS bead hybrids under photo illumination. (b) Raman spectra of the same four positions marked in Figure 3a. (c) Schematic drawing of the electric potential and static forces when a NO_2 molecular absorb on the graphene with PS beads in darkness or (d) with localized light illumination.

DOI: 10.1021/acsomega.8b03540
ACS Omega 2019, 4, 3812−3819

the propagation of SPP waves redistribute electrons in the graphene, which enhances the gas-sensing performance.

Moreover, in a typical semiconductor photocatalytic reaction an electron is excited from the valence band (VB) of the semiconductor into its conduction band (CB) under the irradiation of a laser. In graphene/PS bead hybrids, the photoexcited electrons and holes can transfer to the graphene, which may strengthen the response of the sensor. However, the PS beads typically have a bandgap width of over 4 eV. Thus, the photons of the laser (wavelength of 635 nm) in our experiments are unable to excite electrons from the VB to CB. Figure S9 shows the electric field potentials of a NO_2 molecule in air, on the top of graphene, and near the graphene/PS beads interface. The simulated electric field is pointed from PS beads to the graphene, confirming transfer of electrons from the graphene to the PS beads, which is consistent with experimental observations. In dark conditions, when a NO_2 molecule is near the concave region between the graphene and PS sphere, there are two competing static forces that will drag the NO_2 molecule into the concave shadow regions (Figure 5c). One of the static forces is from the graphene surface and the other is from the PS. Thus, more NO_2 molecules will be aggregated within this concave region and cause a sensitivity increase. After being illuminated with localized light, more electrons will transfer from the graphene to the PS beads and this will result in a small dipole layer appearing in the contact region of the PS spheres and graphene. Thus, NO_2 molecules will be attracted into the concave regions through the dipolar interaction between the dipole layer and NO_2 polar molecules (Figure 5d). This dipolar interaction depends on the dipole layer strength, and should be higher than the induced static interactions in the dark conditions, which further enhances the sensitivity and results in faster adsorption.

3. CONCLUSIONS

To conclude, we have proposed and demonstrated a simple and cheap method to enhance the NO_2-sensing performance of the graphene. An ultra-low DL of 0.5 ppb was determined. The enhanced gas sensing is due to the SPPs excited in the graphene and the charge transfer between the PS beads and graphene. Our results open an interesting route for the application of the graphene in gas sensing.

4. EXPERIMENTAL SECTION

4.1. Sample Preparation and Characterization. Graphene was synthesized on Ar plasma-treated Cu foil (Alfa Aesar, annealed, 0.025 mm thick, 99.8% pure) via CVD. The graphene growth was carried out at 1035 °C for 40 min under a methane and a hydrogen flow. Details of the growth can be found elsewhere. Raman analysis was carried out using a Bruker Raman microscope with an excitation wavelength of 532 nm. SEM characterization was carried out with a FEI Quanta 650 FEG scanning electron microscope. TEM samples were prepared by transferring the as-grown films onto TEM grids. The TEM studies were performed in JEOL JEM-2100 F with a probe size under 0.5 nm, 200 kV.

4.2. Device Fabrication and Measurement. Devices were made by evaporating Ti/Au (10/25 nm) onto the graphene through a shadow mask. The distance between electrodes was between ∼40 μm and ∼1 mm. The gas sensor was tested in a custom-made chamber with remote-controllable mass-flow controllers. All of the sensors were measured at atmospheric pressure and RT. The change in resistance upon different gas exposures was monitored by Keithley 2400A source-meters.

■ ASSOCIATED CONTENT

Supporting Information

The Supporting Information is available free of charge on the ACS Publications website at DOI: 10.1021/acsomega.8b03540.

(a) Optical image and (b) corresponding Raman spectra of the graphene on the Si substrate; magnified gas-sensing dynamics under each gas concentration; dynamic-sensing response of the graphene sensor after PS bead drop-coating measured under 635 nm photoillumination; multicycle responses of the sensor when exposed to 8800 ppb NO_2, low-magnification SEM images; typical photographic image of a device; adsorption time as a function of gas concentration for a variety PS coverage concentration illumination conditions; dynamic-sensing response of four graphene sensors with different PS concentrations; and simulated the electric field of NO_2 molecular on top of graphene, the total electric field of NO_2 molecular equal to the dipole field of NO_2 molecular E_{NO^2} plus the image field of the Graphene/SiO_2 substance E_{sub} . (b) Simulated electric field potentials of NO_2 molecular near the Graphene/PS beads interface, the enhanced electric field of NO_2 molecular due to the image field of PS sphere E_{PS} . (c) Simulated electric field potentials of NO_2 molecular absorbed into the concave of Graphene and PS beads, the effect of E_{PS} is more obvious than (b) (PDF)

■ AUTHOR INFORMATION

Corresponding Authors

*E-mail: crchang@phys.ntu.edu.tw (C.-R.C.).
*E-mail: wuhc@bit.edu.cn (H.-C.W.).

ORCID

Yanhui Chen: 0000-0002-3215-9302
Lei Zhang: 0000-0003-3765-7324
Han-Chun Wu: 0000-0003-0293-9022

Notes

The authors declare no competing financial interest.

■ ACKNOWLEDGMENTS

We are grateful for the help provided Conor Cullen, TCD, in acquiring the XPS spectra. This work was supported by the National Key Research and Development Program under grant nos. 2017YFE0301404 and 2017YFA0303800, the National Natural Science Foundation of China (no. 61874010), the Science and Technology Innovation Program for Creative Talents in Beijing Institute of Technology (no. 2017CX01006), and by Ministry of Science and Technology of R. O. C. under grant No. MOST 107-2112-M-002-013-MY3.

■ REFERENCES

(1) Barea, E.; Montoro, C.; Navarro, J. A. R. Toxic gas removal - metal-organic frameworks for the capture and degradation of toxic gases and vapours. *Chem. Soc. Rev.* **2014**, *43*, 5419−5430.

DOI: 10.1021/acsomega.8b03540
ACS Omega 2019, 4, 3812−3819

(2) Hoa, N. D.; El-Safty, S. A. Synthesis of Mesoporous NiO Nanosheets for the Detection of Toxic NO_2 Gas. *Chem.—Eur. J.* **2011**, *17*, 12896−12901.
(3) Wang, S.; Huang, D.; Xu, S.; Jiang, W.; Wang, T.; Hu, J.; Hu, N.; Su, Y.; Zhang, Y.; Yang, Z. Two-dimensional NiO nanosheets with enhanced room temperature NO_2 sensing performance via Al doping. *Phys. Chem. Chem. Phys.* **2017**, *19*, 19043−19049.
(4) Lu, G.; Xu, J.; Sun, Y.; Yu, Y.; Zhang, Y.; Liu, F. UV-enhanced room temperature NO_2 sensor using ZnO nanorods modified with SnO_2 nanoparticles. *Sens. Actuators, B* **2012**, *162*, 82−88.
(5) Kida, T.; Nishiyama, A.; Hua, Z.; Suematsu, K.; Yuasa, M.; Shimanoe, K. WO_3 Nano lamella Gas Sensor: Porosity Control Using SnO_2 Nanoparticles for Enhanced NO_2 Sensing. *Langmuir* **2014**, *30*, 2571−2579.
(6) Zhang, D.; Liu, Z.; Li, C.; Tang, T.; Liu, X.; Han, S.; Lei, B.; Zhou, C. Detection of NO_2 down to ppb levels using individual and multiple In_2O_3 nanowire devices. *Nano Lett.* **2004**, *4*, 1919−1924.
(7) Dai, Z.; Lee, C.-S.; Tian, Y.; Kim, I.-D.; Lee, J.-H. Highly reversible switching from P- to N-type NO_2 sensing in a monolayer Fe_2O_3 inverse opal film and the associated P-N transition phase diagram. *J. Mater. Chem. A* **2015**, *3*, 3372−3381.
(8) Deng, S.; Tjoa, V.; Fan, H. M.; Tan, H. R.; Sayle, D. C.; Olivo, M.; Mhaisalkar, S.; Wei, J.; Sow, C. H. Reduced Graphene Oxide Conjugated Cu_2O Nanowire Mesocrystals for High-Performance NO_2 Gas Sensor. *J. Am. Chem. Soc.* **2012**, *134*, 4905−4917.
(9) Kumar, R.; Al-Dossary, O.; Kumar, G.; Umar, A. Zinc Oxide Nanostructures for NO_2 Gas-Sensor Applications: A Review. *Nano-Micro Lett.* **2014**, *7*, 97−120.
(10) Virji, S.; Huang, J.; Kaner, R. B.; Weiller, B. H. Polyaniline nanofiber gas sensors: Examination of response mechanisms. *Nano Lett.* **2004**, *4*, 491−496.
(11) Talwar, V.; Singh, O.; Singh, R. C. ZnO assisted polyaniline nanofibers and its application as ammonia gas sensor. *Sens. Actuators, B* **2014**, *191*, 276−282.
(12) Panes-Ruiz, L. A.; Shaygan, M.; Fu, Y.; Liu, Y.; Khavrus, V.; Oswald, S.; Gemming, T.; Baraban, L.; Bezugly, V.; Cuniberti, G. Toward Highly Sensitive and Energy Efficient Ammonia Gas Detection with Modified Single-Walled Carbon Nanotubes at Room Temperature. *ACS Sens.* **2017**, *3*, 79−86.
(13) Zhang, J.; Liu, X.; Neri, G.; Pinna, N. Nanostructured Materials for Room-Temperature Gas Sensors. *Adv. Mater.* **2015**, *28*, 795−831.
(14) An, K. H.; Jeong, S. Y.; Hwang, H. R.; Lee, Y. H. Enhanced sensitivity of a gas sensor incorporating single-walled carbon nanotube-polypyrrole nanocomposites. *Adv. Mater.* **2004**, *16*, 1005−1009.
(15) Novoselov, K. S.; Geim, A. K.; Morozov, S. V.; Jiang, D.; Zhang, Y.; Dubonos, S. V.; Grigorieva, I. V.; Firsov, A. A. Electric Field Effect in Atomically Thin Carbon Films. *Science* **2004**, *306*, 666.
(16) Geim, A. K.; Novoselov, K. S. The rise of graphene. *Nat. Mater.* **2007**, *6*, 183−191.
(17) Schedin, F.; Geim, A. K.; Morozov, S. V.; Hill, E. W.; Blake, P.; Katsnelson, M. I.; Novoselov, K. S. Detection of individual gas molecules adsorbed on graphene. *Nat. Mater.* **2007**, *6*, 652−655.
(18) Yuan, W.; Shi, G. Graphene-based gas sensors. *J. Mater. Chem. A* **2013**, *1*, 10078−10091.
(19) Xia, Y.; Li, R.; Chen, R.; Wang, J.; Xiang, L. 3D Architectured Graphene/Metal Oxide Hybrids for Gas Sensors: A Review. *Sensors* **2018**, *18*, 1456−1476.
(20) Yavari, F.; Castillo, E.; Gullapalli, H.; Ajayan, P. M.; Koratkar, N. High sensitivity detection of NO_2 and NH_3 in air using chemical vapor deposition grown graphene. *Appl. Phys. Lett.* **2012**, *100*, 203120.
(21) Seekaew, Y.; Lokavee, S.; Phokharatkul, D.; Wisitsoraat, A.; Kerdcharoen, T.; Wongchoosuk, C. Low-cost and flexible printed graphene-PEDOT:PSS gas sensor for ammonia detection. *Org. Electron.* **2014**, *15*, 2971−2981.
(22) Kumar, R.; Varandani, D.; Mehta, B. R.; Singh, V. N.; Wen, Z.; Feng, X.; Müllen, K. Fast response and recovery of hydrogen sensing in Pd-Pt nanoparticle-graphene composite layers. *Nanotechnology* **2011**, *22*, 275719.
(23) Pearce, R.; Iakimov, T.; Andersson, M.; Hultman, L.; Spetz, A. L.; Yakimova, R. Epitaxially grown graphene based gas sensors for ultra sensitive NO_2 detection. *Sens. Actuators, B* **2011**, *155*, 451−455.
(24) Choi, H.; Jeong, H. Y.; Lee, D.-S.; Choi, C.-G.; Choi, S.-Y. Flexible NO_2 gas sensor using multilayer graphene films by chemical vapor deposition. *Carbon Lett.* **2013**, *14*, 186−189.
(25) Chung, M. G.; Kim, D. H.; Lee, H. M.; Kim, T.; Choi, J. H.; Seo, D. k.; Yoo, J.-B.; Hong, S.-H.; Kang, T. J.; Kim, Y. H. Highly sensitive NO_2 gas sensor based on ozone treated graphene. *Sens. Actuators, B* **2012**, *166−167*, 172−176.
(26) Zhang, Y.-H.; Chen, Y.-B.; Zhou, K.-G.; Liu, C.-H.; Zeng, J.; Zhang, H.-L.; Peng, Y. Improving gas sensing properties of graphene by introducing dopants and defects: a first-principles study. *Nanotechnology* **2009**, *20*, 185504.
(27) Kaniyoor, A.; Jafri, R. I.; Arockiadoss, T.; Ramaprabhu, S. Nanostructured Pt decorated graphene and multi walled carbon nanotube based room temperature hydrogen gas sensor. *Nanoscale* **2009**, *1*, 382−386.
(28) Gutés, A.; Hsia, B.; Sussman, A.; Mickelson, W.; Zettl, A.; Carraro, C.; Maboudian, R. Graphene decoration with metal nanoparticles: Towards easy integration for sensing applications. *Nanoscale* **2012**, *4*, 438−440.
(29) Huang, W. C.; Tsai, H. J.; Lin, T. C.; Weng, W. C.; Chang, Y. C.; Chiu, J. L.; Lin, J.-J.; Lin, C. F.; Lin, Y.-S.; Chen, H. Incorporation of carbon nanotube and graphene in ZnO nanorods-based hydrogen gas sensor. *Ceram. Int.* **2018**, *44*, 12308−12314.
(30) Li, Z.; Liu, Y.; Guo, D.; Guo, J.; Su, Y. Room-temperature synthesis of Cuo/reduced graphene oxide nanohybrids for high-performance NO_2 gas sensor. *Sens. Actuators, B* **2018**, *271*, 306−310.
(31) Achary, L. S. K.; Kumar, A.; Barik, B.; Nayak, P. S.; Tripathy, N.; Kar, J. P.; Dash, P. Reduced graphene oxide-$CuFe_2O_4$ nano-composite: A highly sensitive room temperature NH3 gas sensor. *Sens. Actuators, B* **2018**, *272*, 100−109.
(32) Parmar, M.; Balamurugan, C.; Lee, D.-W. PANI and Graphene/PANI Nanocomposite Films - Comparative Toluene Gas Sensing Behavior. *Sensors* **2013**, *13*, 16611−16624.
(33) Mishra, S. K.; Tripathi, S. N.; Choudhary, V.; Gupta, B. D. SPR based fibre optic ammonia gas sensor utilizing nanocomposite film of PMMA/reduced graphene oxide prepared by in situ polymerization. *Sens. Actuators, B* **2014**, *199*, 190−200.
(34) Hong, J.; Lee, S.; Seo, J.; Pyo, S.; Kim, J.; Lee, T. A Highly Sensitive Hydrogen Sensor with Gas Selectivity Using a PMMA Membrane-Coated Pd Nanoparticle/Single-Layer Graphene Hybrid. *ACS Appl. Mater. Interfaces* **2015**, *7*, 3554−3561.
(35) Liu, X.; Zhang, D.; Wu, Y.-C.; Yang, M.; Wang, Q.; Coileáin, C. Ó.; Xu, H.; Yang, C.; Abid, M.; Abid, M.; Liu, H.; Chun, B. S.; Shi, Q.; Wu, H.-C. Ultra-sensitive graphene based mid-infrared plasmonic bio-chemical sensing using dielectric beads as a medium. *Carbon* **2017**, *122*, 404−410.
(36) Chen, S.; Ji, H.; Chou, H.; Li, Q.; Li, H.; Suk, J. W.; Piner, R.; Liao, L.; Cai, W.; Ruoff, R. S. Millimeter-Size Single-Crystal Graphene by Suppressing Evaporative Loss of Cu During Low Pressure Chemical Vapor Deposition. *Adv. Mater.* **2013**, *25*, 2062−2065.
(37) Chen, Y.; Meng, L.; Zhao, W.; Liang, Z.; Wu, X.; Nan, H.; Wu, Z.; Huang, S.; Sun, L.; Wang, J.; Ni, Z. Raman mapping investigation of chemical vapor deposition-fabricated twisted bilayer graphene with irregular grains. *Phys. Chem. Chem. Phys.* **2014**, *16*, 21682−21687.
(38) Chen, G.; Paronyan, T. M.; Pigos, E. M.; Harutyunyan, A. R. Enhanced gas sensing in pristine carbon nanotubes under continuous ultraviolet light illumination. *Sci. Rep.* **2012**, *2*, 343.
(39) Su, Z.; Tan, L.; Yang, R.; Zhang, Y.; Tao, J.; Zhang, N.; Wen, F. Cu-modified carbon spheres/reduced graphene oxide as a high sensitivity of gas sensor for NO_2 detection at room temperature. *Chem. Phys. Lett.* **2018**, *695*, 153−157.
(40) Cui, S.; Pu, H.; Mattson, E. C.; Wen, Z.; Chang, J.; Hou, Y.; Hirschmugl, C. J.; Chen, J. Ultrasensitive Chemical Sensing through Facile Tuning Defects and Functional Groups in Reduced Graphene Oxide. *Anal. Chem.* **2014**, *86*, 7516−7522.

DOI: 10.1021/acsomega.8b03540
ACS Omega 2019, 4, 3812−3819

(41) Bang, J. H.; Choi, M. S.; Mirzaei, A.; Kwon, Y. J.; Kim, S. S.; Kim, T. W.; Kim, H. W. Selective NO_2 sensor based on Bi_2O_3 branched SnO_2 nanowires. *Sens. Actuators, B* **2018**, *274*, 356−369.
(42) Wan, S.; Shao, Z.; Zhang, H.; Yang, Y.; Shao, Z.; Wan, N.; Sun, L. Graphene-based gas sensor. *Chin. Sci. Bull.* **2017**, *62*, 3121−3133.
(43) Jones, C. H.; Wesley, I. J. A preliminary-study of the fourier-transform raman-spectra of polystyrenes. *Spectrochim. Acta, Part A* **1991**, *47*, 1293−1298.
(44) Wu, J.; Xu, H.; Zhang, J. Raman Spectroscopy of Graphene. *Acta Chim. Sin.* **2014**, *72*, 301−318.
(45) Luan, Y.; Zhang, S.; Nguyen, T. H.; Yang, W.; Noh, J.-S. Polyurethane sponges decorated with reduced graphene oxide and silver nanowires for highly stretchable gas sensors. *Sens. Actuators, B* **2018**, *265*, 609−616.
(46) Park, H. J.; Kim, W.-J.; Lee, H.-K.; Lee, D.-S.; Shin, J.-H.; Jun, Y.; Yun, Y. J. Highly flexible, mechanically stable, and sensitive NO_2 gas sensors based on reduced graphene oxide nanofibrous mesh fabric for flexible electronics. *Sens. Actuators, B* **2018**, *257*, 846−852.
(47) Hoa, L. T.; Tien, H. N.; Luan, V. H.; Chung, J. S.; Hur, S. H. Fabrication of a novel 2D-graphene/2D-NiO nanosheet-based hybrid nanostructure and its use in highly sensitive NO_2 sensors. *Sens. Actuators, B* **2013**, *185*, 701−705.
(48) Huang, J.; Xie, G.; Zhou, Y.; Xie, T.; Tai, H.; Yang, G. Polyvinylpyrrolidone/reduced graphene oxide nanocomposites thin films coated on quartz crystal microbalance for NO_2 detection at room temperature. *7th International Symposium on Advanced Optical Manufacturing and Testing Technologies: Smart Structures and Materials for Manufacturing and Testing*; Luo, X., Giessen, H., Eds., 2014; Vol. *9285*.
(49) Huang, L.; Wang, Z.; Zhang, J.; Pu, J.; Lin, Y.; Xu, S.; Shen, L.; Chen, Q.; Shi, W. Fully Printed, Rapid-Response Sensors Based on Chemically Modified Graphene for Detecting NO_2 at Room Temperature. *ACS Appl. Mater. Interfaces* **2014**, *6*, 7426−7433.
(50) Liu, S.; Yu, B.; Zhang, H.; Fei, T.; Zhang, T. Enhancing NO_2 gas sensing performances at room temperature based on reduced graphene oxide-ZnO nanoparticles hybrids. *Sens. Actuators, B* **2014**, *202*, 272−278.
(51) Piloto, C.; Notarianni, M.; Shafiei, M.; Taran, E.; Galpaya, D.; Yan, C.; Motta, N. Highly NO_2 sensitive caesium doped graphene oxide conductometric sensors. *Beilstein J. Nanotechnol.* **2014**, *5*, 1073−1081.
(52) Su, P.-G.; Shieh, H.-C. Flexible NO_2 sensors fabricated by layer-by-layer covalent anchoring and in situ reduction of graphene oxide. *Sens. Actuators, B* **2014**, *190*, 865−872.

DOI: 10.1021/acsomega.8b03540
ACS Omega 2019, 4, 3812−3819